IEEE Access
Multidisciplinary | Rapid Review | Open Access Journal

Received February 22, 2021, accepted March 20, 2021, date of publication March 24, 2021, date of current version April 7, 2021.

Digital Object Identifier 10.1109/ACCESS.2021.3068653

Voltage Oriented Controller Based Vienna Rectifier for Electric Vehicle Charging Stations

GOWTHAMRAJ RAJENDRAN[1], CHOCKALINGAM ARAVIND VAITHILINGAM[1], (Senior Member, IEEE), NORHISAM MISRON[2,3,4], (Member, IEEE), KANENDRA NAIDU[5], AND MD RISHAD AHMED[6]

[1]High Impact Research Laboratory, Faculty of Innovation and Technology, School of Computer Science and Engineering, Taylor's University, Subang Jaya 47500, Malaysia
[2]Faculty of Engineering, Universiti Putra Malaysia, Serdang 43400, Malaysia
[3]Institute of Advance Technology (ITMA), Universiti Putra Malaysia, Serdang 43400, Malaysia
[4]Institute of Plantation Studies, Universiti Putra Malaysia, Serdang 43400, Malaysia
[5]Faculty of Electrical Engineering, Universiti Teknologi MARA (UiTM), Shah Alam 40450, Malaysia
[6]Department of Electrical and Electronic Engineering, University of Nottingham, Nottingham NG7 2RD, U.K.

Corresponding authors: Chockalingam Aravind Vaithilingam (aravindcv@ieee.org) and Norhisam Misron (norhisam@upm.edu.my)

This work was supported in part by the Taylor's University through its Taylor's Research Scholarship Programme under Grant TUFR/2017/001/01, and in part by the Article Publication Charges (APCs) through the University Putra Malaysia (UPM), Malaysia.

ABSTRACT Vienna rectifiers have gained popularity in recent years for AC to DC power conversion for many industrial applications such as welding power supplies, data centers, telecommunication power sources, aircraft systems, and electric vehicle charging stations. The advantages of this converter are low total harmonic distortion (THD), high power density, and high efficiency. Due to the inherent current control loop in the voltage-oriented control strategy proposed in this paper, good steady-state performance and fast transient response can be ensured. The proposed voltage-oriented control of the Vienna rectifier with a PI controller (VOC-VR) has been simulated using MATLAB/Simulink. The simulations indicate that the input current THD of the proposed VOC-VR system was below 3.27% for 650V and 90A output, which is less than 5% to satisfy the IEEE-519 standard. Experimental results from a scaled-down prototype showed that the THD remains below 5% for a wide range of input voltage, output voltage, and loading conditions (up to 2 kW). The results prove that the proposed rectifier system can be applied for high power applications such as DC fast-charging stations and welding power sources.

INDEX TERMS Front-end converters, high power applications, power factor, total harmonic distortion, Vienna rectifier, voltage oriented controller.

I. INTRODUCTION

AC to DC converters with regulated DC output voltage is used as front-end converters for different applications such as electric vehicle chargers, telecommunication applications, welding power sources, data center, and motor drives [1], [2]. The power required for EV charging stations and welding power sources is high, which means that the voltage and current rating at the power converters must be higher than the voltage and current required for other applications such as motor traction [3], [4]. The unidirectional boost rectifier known as Vienna rectifier is used as a front-end converter [5]. This converter is well known for its topological structure advantages such as high efficiency, high power to weight ratio, low total harmonic distortion in the line current, unity power factor at the grid, and the small size of the filter compared to conventional three-phase rectifiers [6]. The Vienna rectifier is ideal for high power applications owing to the high power to weight ratio, high efficiency, and low voltage stress [7], [8].

In recent years, the core of the power electronics systems is the controller unit, which has been subjected to intensive research. The basic controller used in a power converter is a proportional-integral (PI) controller. However, it is challenging to achieve an accurate linear mathematical model of the system required for the PI controller [9]. Moreover, the PI controller often struggles to work satisfactorily under parameter variations, nonlinearity, and load disturbances [10].

The associate editor coordinating the review of this manuscript and approving it for publication was Yijie Wang.

TABLE 1. Comparison of different controllers.

Ref.	Power converter	Power controller	% THD	Remarks
[15]	Diode-Bridge rectifier	PFC controller Current Controller	6.22	This converter is connected to the Buck-Boost converter for EV charging applications.
[16]	SEPIC Converter	Genetic Algorithm based PFC controller	1.68	This system is controlled by an intelligent controller, which improves the settling time. (Settling time = 0.3s).
[17]	Three-phase diode bridge rectifier	Direct Power Controller (DPC)	2.01	The power converter is used for low-power DC applications.
[12]	Three-phase controlled rectifier	DPC controller	4.6	The power converters are used for renewable energy applications.
[18]	Inverter	DPC controller	6.4	The DPC controller regulates the grid side voltage in inverter applications.
[19]	Three-phase controlled rectifier	Voltage Oriented Controller	0.28	The VOC controller with a fuzzy logic controller is used for induction motor drive applications
[14]	Three-phase controlled rectifier	DPC-SVM	4	This controller is used for Induction motor applications.

In literature, different control methods are used in AC to DC converters for high power applications such as welding power sources and electric vehicle charging stations. The most popular power controllers for EV charging stations are power factor correction controllers (PFC) [11], direct power controller (DPC) [12], voltage-oriented controller (VOC) [13], and their combination DPC-SVM [14]. Voltage oriented controller is commonly used as a power controller for power factor correction in active front-end converters. Table 1 shows the comparison of different controllers.

Table 1 demonstrates the combination of a conventional controller with an intelligent controller can improve the transient analysis of the system and reduce total harmonic distortion in the input current compared to an individual controller. Furthermore, different converters used in the literature are applicable to lower power DC applications and traction applications.

In this paper, a novel design of EV charging system consisting of voltage-oriented controller with a Vienna rectifier (VOC-VR) is proposed for high power applications. The proposed system is a hybrid control structure consisting of voltage-oriented controller with PI controller for the Vienna rectifier, which is used for EV charging stations. Prior designs of AC/DC converters for high power applications employed a hybrid controller using conventional three-phase controlled

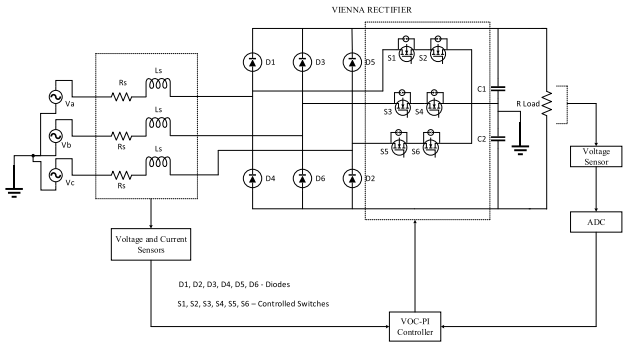

FIGURE 1. The proposed electric vehicle charger is based on Vienna rectifier with a VOC controller (VOC-VR) system.

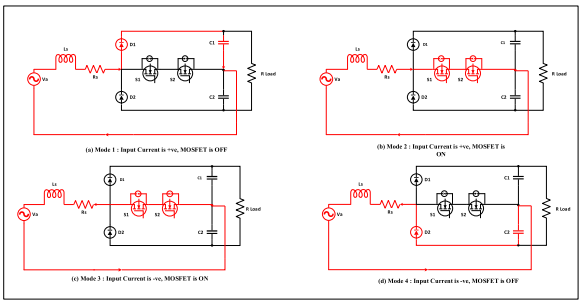

FIGURE 2. Four modes of operation of Vienna rectifier topology.

rectifiers, which requires input and output filters with high rating to mitigate the input current THD [13], [14], [16], [20]. This led to reduced efficiency and power density of the system. To address this issue, a novel design of integrating Vienna rectifier with a VOC and PI controller for high power applications is proposed. Using Vienna rectifier, transient stability is improved, and for an output voltage of 650 V/ 90 A, the THD is reduced to less than 5%, which satisfies the IEEE-519 standard. The proposed novel design outperforms existing AC/DC power converters for high power applications by significantly reducing the input current THD and increasing the power density.

II. VIENNA RECTIFIER

The Vienna rectifier topology includes six active semiconductor switches, either MOSFET or IGBT, and six diodes. The three-phase three-level Vienna rectifier topology is shown in Fig. 1. The voltage stress on each diode and semiconductor switches is $V_{dc}/2$. Three inductors on the input AC side and two capacitors are parallelly connected on the DC side. The neutral point of the grid is associated with the neutral point of the DC link. Fig. 2 shows the operation of the three-level Vienna rectifier for the current path of one leg at each mode. The remaining two legs perform the same operation with a 120° phase difference.

In mode 1, when a reference voltage is a positive half cycle and controlled switches (IGBTs/MOSFETs) are OFF, the diode D_1 conducts. During this time, the current flows through $V_a L_s R_s D_1 C_1$ as shown in Fig. 2(a). In mode 2 operation, when a reference voltage is positive half cycle with

controlled switches are ON, switches S_1S_2 conducts and current flows through $V_aL_sR_sS_1S_2$ as shown in Fig. 2(b). In mode 3 operations, when a reference voltage is negative half cycle with controlled switches are ON, switches S_1S_2 conducts and the current flows through $S_1S_2R_sL_sV_a$ as shown in Fig. 2(c). In mode 4 operation, when a reference voltage is negative half cycle with controlled switches are OFF, the current flows through $C_2D_2R_sL_sV_a$ as shown in Fig. 2(d).

It is observed from Table 2, Vienna Rectifier is applicable for high power applications such as welding power sources, wind energy conversion systems, electric vehicle charging stations, and telecommunication power sources. Different power controllers have been used in Vienna Rectifier for high power applications, such as vector controller, SVPWM controller, predictive controller, and dead-beat controller. The different types of intelligent controllers have been combined with conventional controllers to improve the stability of the system, which increases the complexity of the system. The proposed system consists of Voltage Oriented Controller for Vienna Rectifier (VOC-VR). The proposed system reduces the harmonics in the input source current, improves the power factor at the grid side, and improves the stability of the system.

III. VOLTAGE ORIENTED CONTROLLER

The operation of AC to DC power converters strongly depends on the implemented control structure. The operation of a voltage-oriented controller is based on dual vector current controllers (DVCC) [31]. Voltage-oriented control is used to mitigate the following problem:

- Output DC voltage ripples
- Total harmonics distortion in the input current
- Input power factor at the grid side

The voltage-oriented controller consists of a voltage controller and a current controller. The current control algorithm has two independent current controllers, which will work in the positive and negative synchronous reference frames (SRF). The positive SRF is used to control the positive current component, which rotates in a clockwise direction, whereas the negative SRF is used to control the negative current component, which rotates in the opposite direction. Since the currents occur as DC values in their frame in SRF, a tracking controller does not need to be built. Due to this advantage, the PI controller is adequate to solve the problems above.

The root of VOC approach is the field-oriented controller (FOC) for induction motors, which offers fast and dynamic responses using current controller loops. The VOC technique used for power electronic converters has been widely known in its theoretical aspects [32]. The pulse width modulation approach is added to the control system to improve the features of the VOC system. The minimization of interference (disturbance) can be done by using the VOC technique. By applying hysteresis Pulse Width Modulation (PWM) technique, the system performance has improved. The variable

TABLE 2. Vienna rectifier and its applications.

Ref.	Power Controller	% THD	Power Factor	Application	Remarks
[21]	SVPWM	3.99	0.98	-	The control technique has strong dynamics of equilibrium. The midpoint fluctuation is minimal, and the current distortion on the source side is eliminated to null.
[22]	Conventional PFC Controller	1.46	0.96	EV Application	The PFC controller is used for low-power applications such as a slow charging station for EVs.
[23]	VC based on hysteresis current control	4	0.96	MEA Application	Vienna Rectifier is used for More Electric Aircraft applications. The conversion efficiency is more than 95%.
[24]	Mixed Signal based Control	4.7	0.98	Onboard EV Charger	The Vienna Rectifier is used for the onboard charger with a 0.99 power factor, 4.7% THD, and 98% efficiency.
[25]	-	-	0.98	EV Battery Charger	SiC-based Vienna Rectifier is used for an EV battery charger. This type of design is used for high-power, high-frequency applications.
[26]	-	-	0.98	EV Charger	The Vienna Rectifier is used for an EV charger with a vector control strategy. High power factor, good dynamic stability, and small midpoint potential fluctuations.
[27]	New Synergetic Vector control	-	0.99	EV Charger	New Synergetic Controller consists of a vector controller that is used to reduce the losses in EV chargers.
[28]	Sensorless Voltage control	1.5	-	Telecommunication Application	The Vienna Rectifier is used for telecommunication applications with sensorless control.
[29]	PC with Space vector	-	-	Wind Energy Applications	The Vienna Rectifier is used as a front-end Wind energy converter.

TABLE 2. ***(Continued.)*** **Vienna rectifier and its applications.**

	modulation			The current ripple is reduced, and the neutral point voltage is regulated by the offset voltage determined by the Vienna rectifier's neutral point voltage model.
[30]	Direct Power Control Strategy	1.84	-	High power applications	The Direct Power Control Strategy for Wind energy system improves the power factor at the source side and reduces the THD to less than 5% to satisfy the IEEE-519 Standards.

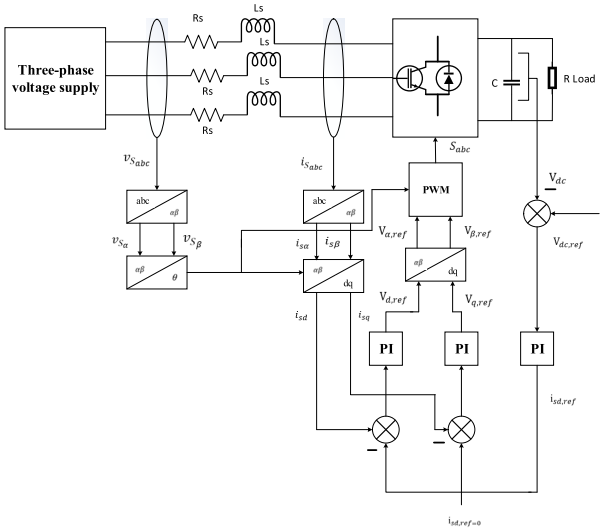

FIGURE 3. **The control structure of voltage-oriented controller with PWM technique.**

switching frequency of the power converters raises the stress in power switching, resulting in large input and output filters.

The proposed approach applies the VOC technology for regulating the charging mechanism with reduced current harmonics in the grid, as shown in Fig. 3. The voltage-oriented controller primarily works in the two-phase $\alpha\beta0$ and dq0 domains where Clark and Park transformation matrices are implemented, as shown in equations (1) and (2), respectively.

$$\begin{bmatrix} v_{s\alpha} \\ v_{s\beta} \\ v_0 \end{bmatrix} = \sqrt{\frac{2}{3}} \begin{bmatrix} 1 & -\frac{1}{2} & -\frac{1}{2} \\ 0 & \frac{\sqrt{3}}{2} & -\frac{\sqrt{3}}{2} \\ \frac{1}{\sqrt{2}} & \frac{1}{\sqrt{2}} & \frac{1}{\sqrt{2}} \end{bmatrix} \begin{bmatrix} v_{sa} \\ v_{sb} \\ v_{sc} \end{bmatrix} \quad (1)$$

$$\begin{bmatrix} v_d \\ v_q \end{bmatrix} = \begin{bmatrix} sin\theta & cos\theta \\ -cos\theta & sin\theta \end{bmatrix} \begin{bmatrix} v_{s\alpha} \\ v_{s\beta} \end{bmatrix} \quad (2)$$

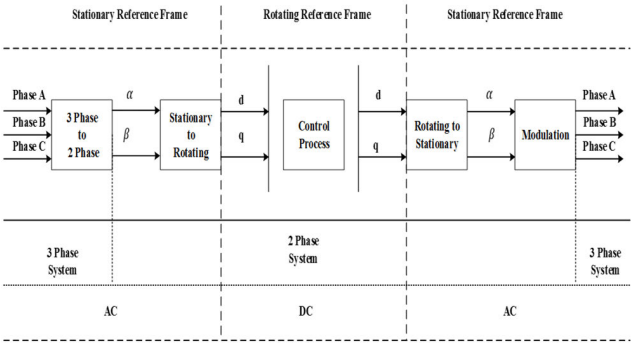

FIGURE 4. **Overall domain transformation sequences involved in the voltage-oriented controller technique.**

where, v_{sa}, v_{sb}, v_{sc} are the three-phase source voltages in the ABC domain, $v_{s\alpha}$, $v_{s\beta}$, v_0, v_d, v_q are the source voltages in the $\alpha\beta0$ and dq0 domains, and θ is the operating phase of the power system. A similar transformation approach is applied to convert the three-phase source current i_{Sabc} as shown in Fig. 3.

AC side control variables become the DC signals by modifying the transformation technique. The proportional-integral controllers easily eliminate steady-state errors according to the following approaches [13]:

$$v_{d,ref} = K_p\left(i_{Sd,ref} - i_{Sd}\right) + K_i(i_{Sd,ref} - i_{Sd})dt \quad (3)$$

$$v_{q,ref} = K_p\left(i_{Sq,ref} - i_{Sq}\right) + K_i(i_{Sq,ref} - i_{Sq})dt \quad (4)$$

K_p and K_i = PI controller gains
i_{Sd} and i_{Sq} = input current in the dq0 domain,
$i_{Sd,ref}$ and $i_{Sq,ref}$ = reference signals for i_{Sd} and i_{Sq}

By applying an inverse park transformation, the operation of the Vienna rectifier has been controlled, as shown in Eq. (5); after obtaining the reference voltage $v_{d,ref}$ and $v_{q,ref}$ which is used to derive the gate switching pulses S_{abc}. The VOC operation involving the overall domain transformation process is summarized in Fig. 4.

$$\begin{bmatrix} v_{\alpha,ref} \\ v_{\beta,ref} \end{bmatrix} = \begin{bmatrix} sin\theta & -cos\theta \\ cos\theta & sin\theta \end{bmatrix} \begin{bmatrix} v_{d,ref} \\ v_{q,ref} \end{bmatrix} \quad (5)$$

The transformation consists of Park's transformations and Clarke's transformation. Clarke's transformation is used to convert the three-phase quantities (phases A, B, C) into the two-phase stationary quantities (α and β). The Park's transformation converts stationary two-phase (α and β) into the rotating reference frame (d and q). Similarly, using the inverse park's transformation technique, the rotating reference frame (d and q) has been converted into a stationary reference frame (α and β). Furthermore, the stationary reference frame is converted into a three-phase AC system using inverse Clarke's transformation technique.

IV. METHODOLOGY

The proposed Vienna rectifier with VOC controller (VOC-VR) is a three-phase three-level rectifier, which is controlled by the voltage-oriented controller algorithm. The

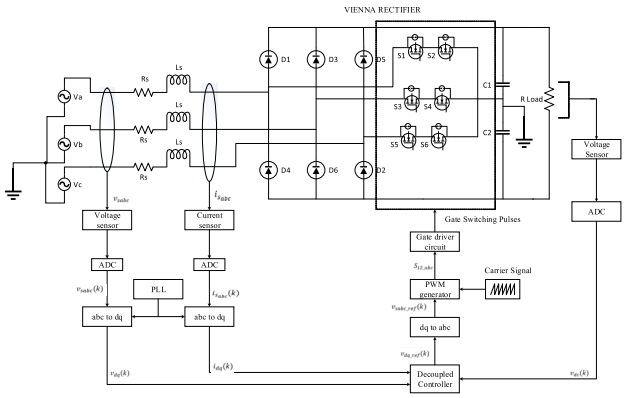

FIGURE 5. Overall Circuit Configuration of the proposed VOC-VR system.

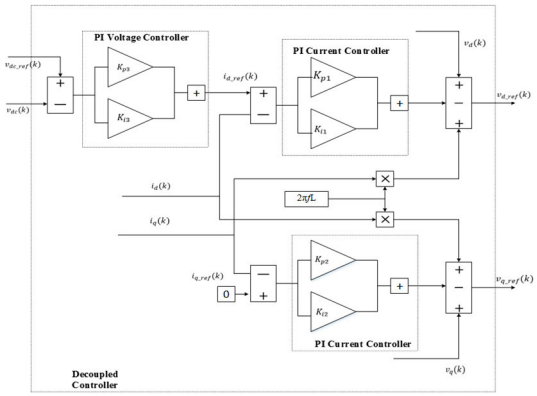

FIGURE 6. The control circuit of the decoupled controller for the voltage-oriented controller technique.

proposed system includes a three-phase AC system, a Vienna rectifier controlled by a VOC algorithm, and a DC link capacitor. Feedback voltage from the EV's load-side battery is generated using current and voltage controllers for the closed-loop operations. The VOC controller performs two main functions: (1) DC output voltage regulation to a pre-determined value, and (2) the regulation of the total input harmonic distortion and maintaining in phase with the voltage to provide unity power factor. The proposed VOC-VR system is shown in Fig. 5.

The de-coupler controller is the key feature of the proposed VOC control algorithm, as shown in Fig. 6. Three PI controllers were used in the proposed control circuit. The first PI controller is a current controller that controls the internal loop of i_d current component. This controller is used to estimate the reference voltage signal v_{d_ref} by minimizing the error between i_d with i_{d_ref}. Second PI controller is also called a PI current controller, which reduces i_q current component to 0 by managing the inner loop of i_q a current component which is used to estimate the voltage reference voltage signal v_{q_ref}. Third PI controller is a voltage controller, which is used to manage the output loop of DC-link voltage V_{dc}. This controller is used to estimate reference current signal i_{d_ref} by comparing measured V_{dc} with its pre-determined reference voltage v_{d_ref}. The voltage-oriented controller must transform input from three-phase current and decouple into active i_d and reactive i_q components, respectively. Regulating the decoupled active and the reactive components minimizes errors between required reference and calculated values of the active and reactive components. The DC link voltage control method controls the active current component i_d which aims to achieve an active power flow balance in the systems while the reactive current component i_q is controlled to 0 to provide a unity power factor at the input side.

The characteristics of two PI current controllers and PI voltage controllers are given in equation (6)-equation (8) [13]

$$v_{d\_ref} = v_d + 2\pi f L_s i_q - (K_{p1}\left(i_{d_{ref}} - i_d\right) + K_{i1}\int \left(i_{d_{ref}} - i_d\right) dt) \quad (6)$$

$$v_{q\_ref} = v_q - 2\pi f L_s i_d - (K_{p2}\left(0 - i_q\right) + K_{i2}\int \left(0 - i_q\right) dt) \quad (7)$$

$$i_{d\_ref} = K_{p3}\left(V_{dc_{ref}} - V_{dc}\right) + K_{i3}\int \left(V_{dc\_ref} - V_{dc}\right) dt \quad (8)$$

$K_{p1}, K_{i1}K_{p2}, K_{i2}K_{p3}, K_{i3}$ = gain values PI current controller
L_s = source inductance.

The switching frequency for the current control loop will be larger than the bandwidth α_i [33],

$$\alpha_i < 2\pi \frac{f_s}{10} \quad (9)$$

$$K_{p1} = K_{p2} = \alpha_i L_s \text{ and } K_{i1} = K_{i2} = \alpha_i R_s \quad (10)$$

where, α_i (rad/s) = current controller bandwidth.

For the voltage control loop, the PI controller is tuned by using a DC link capacitor as the following [34], [35]:

$$K_{p3} \geq C_{dc1}\xi\omega \text{ and } K_{i3} \geq C_{dc1}\xi\omega/2 \quad (11)$$

where damping factor ξ is equal to 0.707 and ω is angular frequency. Using initial values, tuning and modifications are made, which strengthens the proposed charging technique.

V. SIMULATION RESULTS

This section presents the simulation results of a VOC-based Vienna rectifier circuit. The performance of the proposed controller for high-power applications that require 600V/100A DC output is evaluated. The simulation parameters applied for the proposed system are summarized in Table 3.

Vienna rectifier with VOC controller has been simulated in MATLAB Simulink, and results are shown in Fig. 7 and Fig. 8. The input-current waveforms are shown in Fig. 7. The input-current harmonics for Vienna rectifier without a VOC controller and with a VOC controller are shown in Fig. 8 (a) and (b), respectively. From Fig. 7 and Fig. 8, it can be seen that the proposed control technique ensures THD of the input current is less than 3.27%, and the system maintains the unity power factor at the source side. Therefore, the proposed VOC-VR system has been proven to be applicable for

TABLE 3. Specification of a VOC based vienna rectifier (VOC-VR).

Parameter	Symbol	Unit	Value
Resistor Load	R_{load}	Ω	20
Input inductance	L_f	mH	5
Grid frequency	f	Hz	50
Switching frequency	f_s	kHz	12
Input resistance	R_f	Ω	5
Source voltage (AC- RMS)	V_{in}	V	440
Output voltage	V_{dc}	V	600
Current controller	K_{p1} *and* K_{p2}	-	67
Current controller	K_{i1} *and* K_{i2}	-	1.7×10^4
Voltage controller	K_{p3}	-	0.00027
Voltage controller	K_{i3}	-	0.017

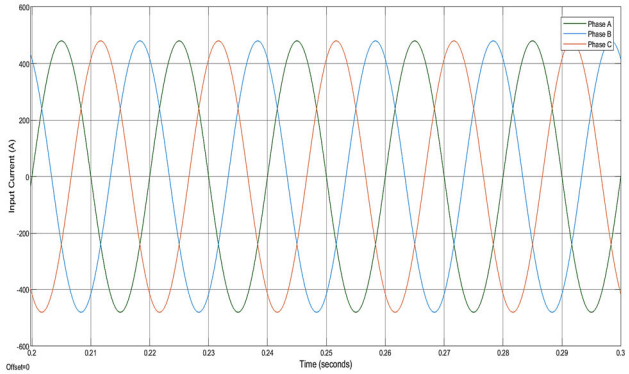

FIGURE 7. Input current waveform of the proposed VOC-VR system with 440 V RMS IN and 650 V DC OUT.

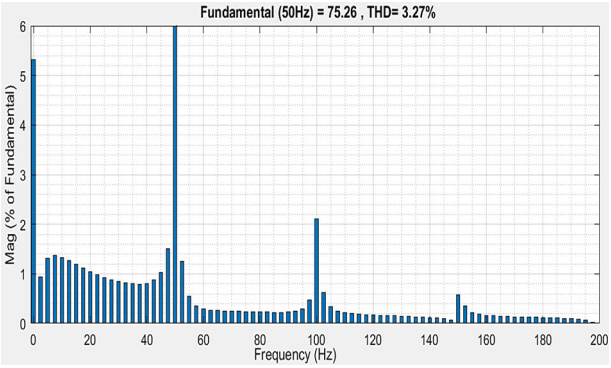

FIGURE 8. Total harmonic distortion of the proposed VOC-VR system with 440 V RMS IN and 650 V DC out.

high power applications with reduced total harmonic distortion to the connected grid. In a previous work [36], Vienna Rectifier with the PFC controller ensured an input current THD of 1.46%. However, the output voltage of the PFC controller with the Vienna rectifier was around 200V, which cannot be used for high power applications such as DC fast chargers for electric vehicles and welding power sources [36]. Hence, voltage-oriented controller with the PWM method for Vienna rectifier gives better performance than the previous work.

Fig 9. shows that the proposed system can maintain the DC output voltage at an optimal level of 650V. The results

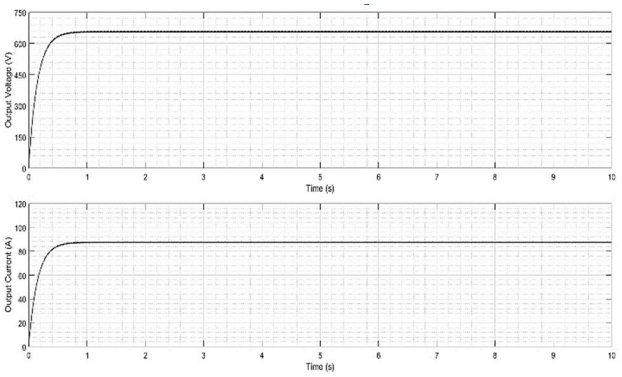

FIGURE 9. DC output voltage and output current of the Vienna rectifier with VOC controller with 350 V AC RMS input and 650 V DC output voltage.

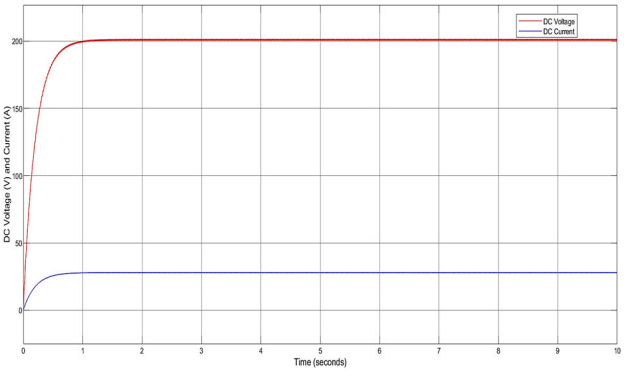

FIGURE 10. DC output voltage and output current of the Vienna rectifier with VOC controller with 350 V AC RMS input and 220 V DC output voltage for slow charging stations.

from this system also show that DC current has been maintained approximately at 90A, which can be used for EV fast charging and welding applications [13]. By scaling down the proposed system and optimizing PI parameters in the VOC controller, the rectifier can be used for slow charging scenarios (250 V/40 A output) as shown in Fig. 10 whereas, the Vienna rectifier with PFC controller can maintain the DC voltage up to 200 V with 16.5 A [36]. As a consequence, the Vienna rectifier with a PFC controller can only be used for slow charging applications (Level 1 charging). The transient analysis has been performed by studying the system performance in the case of an instantaneous increase in the load by a factor of 2. The DC output voltage during the transient condition is shown in Fig. 11.

VI. EXPERIMENT SETUP

A scaled-down demonstrator, the Vienna rectifier board with a resistive load, has been set up to verify the proposed voltage-oriented controller for the Vienna rectifier. The digital controller is preferred due to the limitations of design complexity, slow dynamic response, and high component costs by conventional analog controllers. The digital controller in the proposed system has been developed using a TMS320F28337xD microcontroller. The experimental setup of the proposed system is shown in Fig 12 and 13. It consists

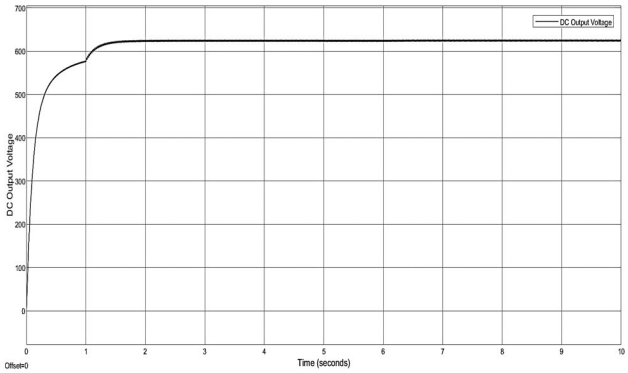

FIGURE 11. DC output voltage for the transient condition during the load variations.

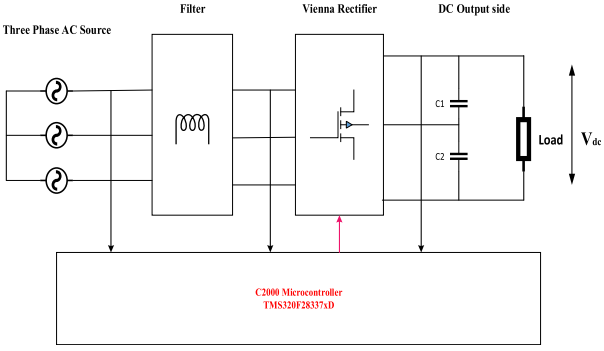

FIGURE 12. Block Diagram of three-phase Vienna Rectifier with a TMS320F28337xD prototype.

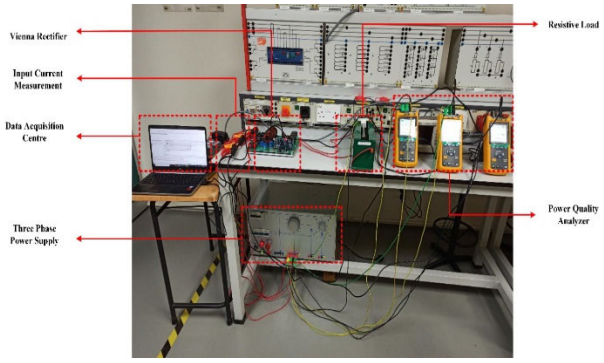

FIGURE 13. The experimental setup of the Vienna Rectifier with a TMS320F28337xD.

of input filters, a Vienna rectifier board, output filters, and a digital controller board. The input voltage and current were measured using a power analyzer. The PCB board of Vienna rectifier with TMS320F28337xD microcontroller is shown in Fig. 14. The MOSFET model used in the rectifier was 65C7190, and the diode model was C4D08120A. The primary filter inductor was 3 mH in each phase, the total output capacitance was 180 μF, and the switching frequency of the rectifier was 50 kHz.

A. INDUCTOR DESIGN

The harmonics in the switching frequency will be reduced by using the input inductor (L_i). Among other considerations,

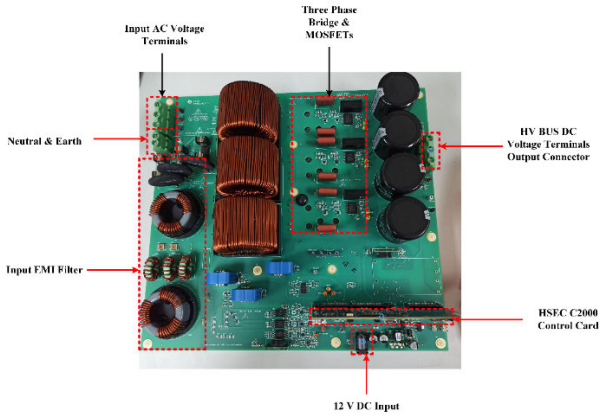

FIGURE 14. Board view of vienna rectifier with TMS320F28337Xd.

the design of the inductor depends on current ripple and the selection of the core material that can withstand the current ripple.

V $= L_i(di/di)$, gives the voltage across the inductor. The voltage equation for Vienna rectifier is,

$$\left(\frac{V_{bus}}{2} - V_{rms}\right) = L_i * \frac{\Delta i_{pp}}{D * T_s} \tag{12}$$

where the time $T_s = 1/F_{sw}$ is switching period, and D is duty cycle. The current ripple Δi_{pp} is,

$$\Delta i_{pp} = \frac{D * T_s * \left(\frac{V_{bus}}{2} - V_{rms}\right)}{L_i} \tag{13}$$

The duty cycle $D = m_a * \sin(\omega t)$, where m_a is the modulation index and input voltage $V_{rms} = D * (V_{bus}/2)$, then current ripple can be derived as,

$$\Delta i_{pp} = \frac{\frac{V_{bus}}{2} * T_s * m_a * \sin(\omega t) * (1 - m_a \sin(\omega t))}{L_i} \tag{14}$$

It is clear from equation 14, the peak ripple changes in a sinusoidal manner. Equation 15 gives the maximum value by differentiating equation 14.

$$\frac{d\left(\Delta i_{pp}\right)}{dt} = K\{\cos(\omega t)(1 - m_a \sin(\omega t)) - m_a \sin(\omega t)\cos(\omega t)\} = 0 \tag{15}$$

At $\sin(\omega t) = 1/(2 * m_a)$, the maximum current ripple has been attained, and it is derived in Equation 16.

$$\Delta i_{pp} = \frac{\frac{V_{bus}}{2} * T_s}{4 * L_i} \tag{16}$$

$$L_i = \frac{\frac{V_{bus}}{2}}{4 * F_{sw} * \Delta i_{pp_{max}}} \tag{17}$$

Using equation (17), required inductance can be calculated, and suitable core material can be selected for inductor design.

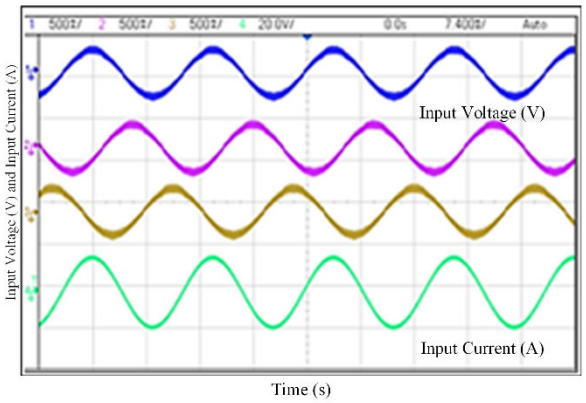

FIGURE 15. Input voltage and current waveforms for 208 V_{AC}, 600V DC, 612W and THD = 2.5%.

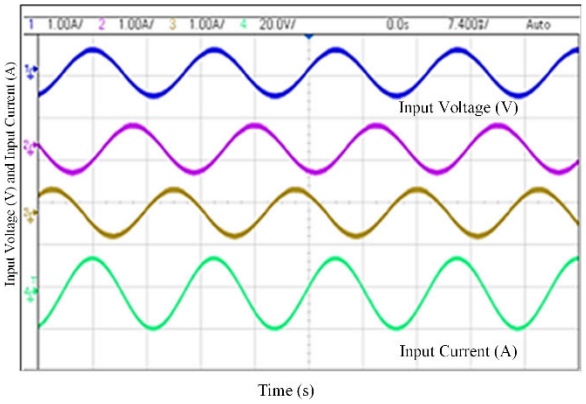

FIGURE 16. Input voltage and current waveforms for 208 V_{AC}, 600V DC, 1364W and THD = 0.96%.

B. OUTPUT CAPACITOR SELECTION

The ripple in the DC output voltage will be minimized by placing a capacitor at the output side. Output capacitor value can be calculated using equation (18) based on the output voltage ripple specification.

$$C = \left(\frac{1}{3}\right) \frac{P_{ac}}{4 * f * \left(V^2 - (V - \Delta V)^2\right)} \tag{18}$$

where,
f = Grid frequency
P_{ac} = AC power (input power) and
ΔV = change in input voltage

VII. EXPERIMENTAL RESULTS

The proposed VOC-based Vienna Rectifier has been experimentally tested to provide constant DC voltage at low input current THD. It is observed from Fig. 15 and 16 that input voltage and current show sinusoidal waveforms when the rectifier was tested with varying load (V_{AC} = 280 *V RMS*). The power measured during these experiments was 612W and 1364 W. The total harmonic distortion for input current was recorded at 2.5% for 612 W operation. The total harmonic distortion for input current was observed 0.96% for 1364 W operation, as shown in Fig.16. The experiments were done

TABLE 4. Experimental results with 208 V_{AC}, 600 V DC output voltage, and varying load.

V_{bus} (V) (AC – RMS)	V_{out} (V)	P_{in} (W)	I_{out} (A)	P_{out} (W)	Efficiency	THD %	PF
300.5	598.5	74	0.117	70.069	0.946	23.20%	0.8623
300	598.35	124.4	0.2	119.16	0.962	17%	0.9203
299.8	598.57	245.1	0.4	239.58	0.977	8.09%	0.9775
299	598.26	481.3	0.788	471.78	0.980	3%	0.997
299.6	598.47	623.2	1.027	612.98	0.981	2.54%	0.995
299.4	598.36	858.6	1.416	841.85	0.980	1.71%	0.994
299.1	598.15	1001.8	1.632	980.46	0.978	1.52%	0.997
299.82	599.8	1150.2	1.878	1125.5	0.978	1.22%	0.998
298.8	598.68	1399.6	2.278	1364.6	0.974	0.96%	0.999

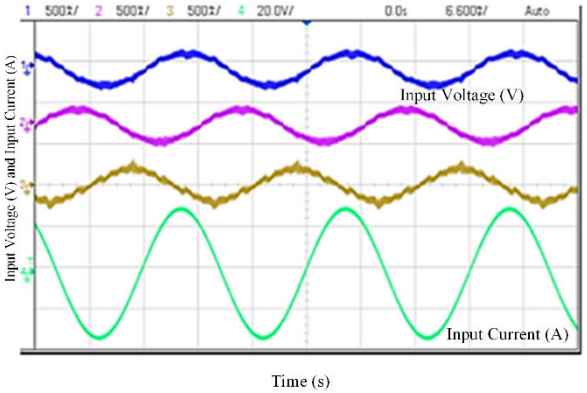

FIGURE 17. Input voltage and current waveforms for 350 V_{AC}, 700V DC, 960W and THD = 7%.

TABLE 5. Experimental results with 350 V_{AC}, 700 V DC output voltage, and varying load.

V_{bus} (V) (AC – RMS)	V_{out} (V)	P_{in} (W)	I_{out} (A)	P_{out} (W)	Efficiency	THD %	PF
351.2	700.41	101.7	0.136	95.86	0.9419	29.10	0.7516
351.7	701.61	265.8	0.38	259.74	0.9779	22	0.9319
352	701.87	581.3	0.829	574.82	0.9862	11.29	0.9832
351.6	701.56	900.6	1.28	890.65	0.9878	7	0.9936
351.9	701.64	1094.5	1.573	1082.24	0.9876	6.23	0.9964
351.7	701.37	1354.4	1.942	1341.53	0.9917	5.46	0.9952
351.4	701.28	1558.3	2.214	1535.46	0.9876	4.80	0.9968
351.2	700.86	1884.7	2.56	1864.98	0.9884	3.50	0.9984

for an input voltage of 350 V_{AC} and output voltage of 700V DC. In these tests, the recorded total harmonics distortion of input current was 7% for the output power of 960W and 3.5% for the output power of 1865W, as shown in Fig. 17 and Fig. 18, respectively. As input current THD is less than 5% in most cases, the IEEE-519 standard is satisfied, and the system provides a good power factor at the input side. The DC voltage at the output side is constant, and it is maintained at 600 V or 700 V – similar to the reference voltage. Table 4 demonstrates the experimental results of the Vienna rectifier with a VOC controller for the input voltage of 208 V AC RMS and output voltage of 600 V DC. The tests were carried out for different load conditions. The DC output voltage is shown in Fig. 19.

Table 5 demonstrates the experimental results of the Vienna rectifier with a VOC controller for the input voltage of 350 V AC RMS with 700 V DC output voltage. The

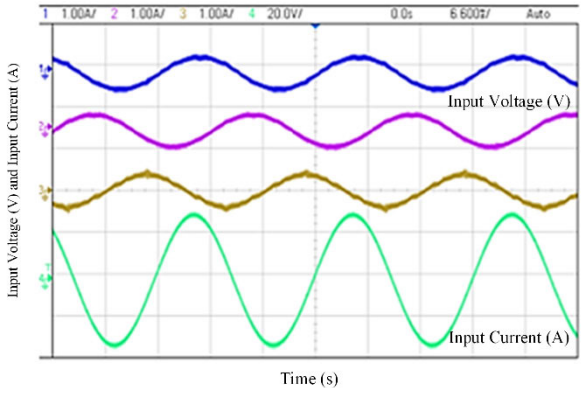

FIGURE 18. Input voltage and current waveforms for 350 V_{AC}, 700V DC, 1865W and THD = 3.5%.

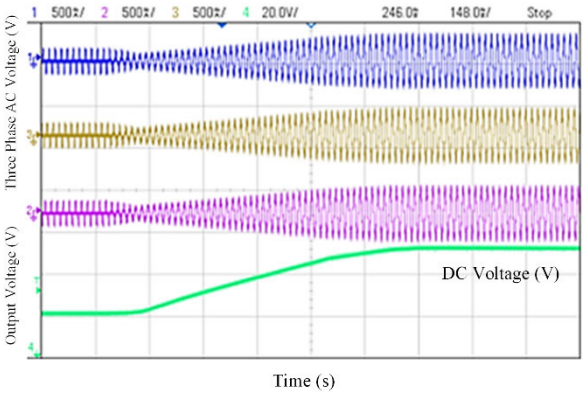

FIGURE 19. DC output voltage of 600 V DC with 612W load.

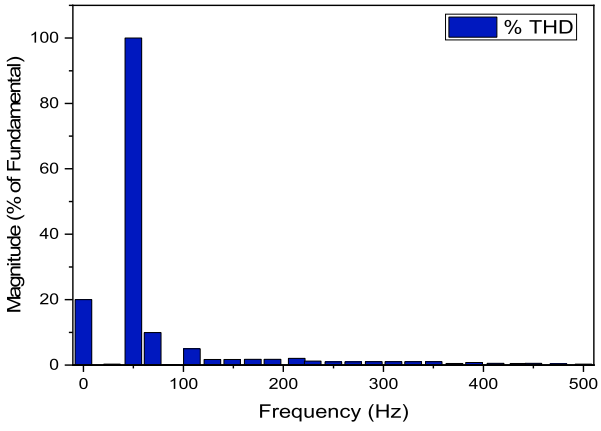

FIGURE 20. Input current THD in % for 350 V AC RMS in and 700V DC out with 1865W.

test results are carried out with different load conditions. Harmonics in the experimental input current for 350 V AC RMS and 700 V DC output are shown in Fig. 20. From Fig. 20, it can be observed that the odd harmonics in the input current have been eliminated [37], which will reduce the size of the filtering components. This again proves that the efficiency of the overall system has been improved with the VOC controller.

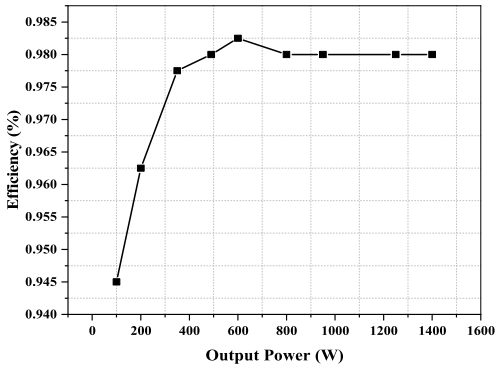

FIGURE 21. Output power vs. efficiency for 350V AC-RMS IN and 700V DC out.

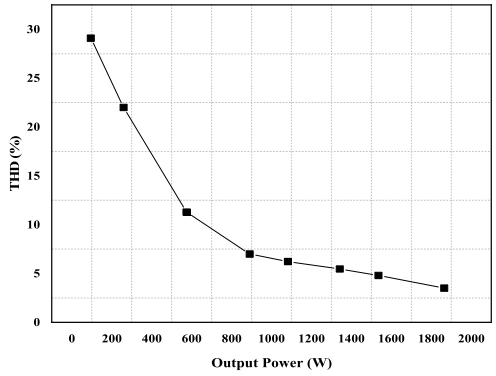

FIGURE 22. Output power vs. % THD for 350V AC-RMS IN and 700V DC out.

Experimental power output vs. efficiency is shown in Fig. 21. The efficiency is maintained above 95% for the different power ratings.

Experimental power output vs. input current THD is shown in Fig. 22. The input current THD is less than 5% for most of the cases. Hence, the input current THD satisfies the IEEE-519.

Experimental power output vs. power factor is shown in Fig. 23. Power factor is maintained between 0.8 and 1 for different loading conditions. The power factor for the proposed system achieves unity for the majority of loading conditions, 200W – 1500W.

VIII. BENCHMARKING

The proposed VOC-based Vienna rectifier (VOC-VR) system improves the rectifier designs from the past works. Table 6 provides a comparison between the proposed system and the published rectifier systems for similar applications. The SEPIC converters and 3 phase-controlled converters are used for medium power applications, for example, wind power applications [38], [39]. The Vienna rectifier with the PFC controller has been used in low-power applications, including slow charging stations for electric vehicles. The voltage produced by the conventional PFC controller-based Vienna rectifier was approximately 200V DC, which is less than the proposed system [36]. This is mainly because the

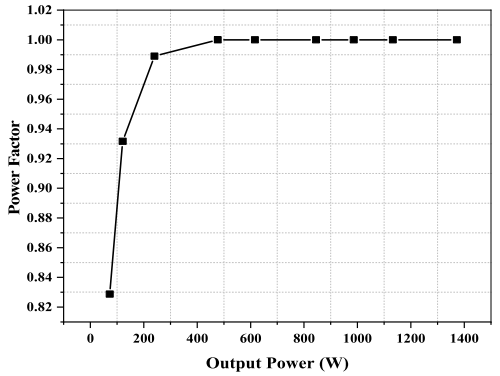

FIGURE 23. Output power vs. power Factor for 350VAC IN and 700V DC OUT.

TABLE 6. The performance of the proposed system compared with existing systems.

Power Converter	Power Controller	Control Structure	%THD	Application
SEPIC Converter [38]	Adaptive Neuro Fuzzy-logic Controller for single-phase PFC controller	Very complex	1.68	This system is used for medium power applications.
Three-phase controlled rectifier [39]	Direct Power Controller	Complex	4.6	This system is used for wind energy applications
Vienna rectifier [36]	PFC controller	Simple	1.46	Low power application such as slow charging stations
Proposed System (VOC – VR)	Voltage Oriented Controller	Simple	3.25	This system is used for high power applications such as DC fast charging station and welding power application

optimization of PI parameters in a conventional PFC controller is challenging for higher output voltage. The optimized PI parameters in the VOC controller give much better results compared to the PFC controller. Hence, the PFC controller-based Vienna rectifier system cannot be used in high-power applications like welding power sources or fast-charging DC stations.

Moreover, the results show that design process of the proposed system is much simpler and use of VOC with the PWM modulator is ideal for specified applications such as EV charging stations and welding power. Using same input filter proposed in the VOC-VR system, the conventional Vienna rectifier designed for high-power applications could increase the input current distortion. Therefore, in order to minimize the total harmonic distortion in input current, the VOC-based PWM control is proposed for the Vienna rectifier.

The simulation and experiment results show that the average input currents THD is less than 5% for most of the cases in the VOC-VR system. In other words, when the proposed system is used in EV fast-charging stations or welding power applications, it will not cause much distortions in the input current, and input power factor would be close to unity.

IX. CONCLUSION

In this research work, a three-level Vienna rectifier based on a voltage-oriented controller (VOC-VR) has been designed and experimentally tested. The proposed system has been simulated using MATLAB Simulink software targeting high-power applications such as DC-fast chargers for electric vehicles. The proposed controller for Vienna rectifier focused on combining voltage-oriented controllers with the PWM method. In proposed design, the reactive and unstable active currents are counteracted by the input and output filters and Voltage Oriented Controller (VOC) with Vienna rectifier. The proposed design also guarantees a sinusoidal current at the input side with minimum ripples and distortions. The system's power factor is maintained at unity, and total harmonic distortion of the input current is kept less than 5 %, which meets the IEEE-519 standard. The benefit of the proposed controller over conventional PFC controller has been demonstrated by simulations and experimental results. Low THD, good power factor, and smaller filtering requirements make the voltage-oriented controller-based Vienna rectifier an ideal candidate in electric vehicle charging stations.

CONFLICT OF INTEREST STATEMENT

On behalf of all authors, the corresponding author states that there is no conflict of interest.

REFERENCES

[1] F. Nejabatkhah, Y. W. Li, and H. Tian, "Power quality control of smart hybrid AC/DC microgrids: An overview," *IEEE Access*, vol. 7, pp. 52295–52318, 2019.

[2] P. Arboleya, G. Diaz, and M. Coto, "Unified AC/DC power flow for traction systems: A new concept," *IEEE Trans. Veh. Technol.*, vol. 61, no. 6, pp. 2421–2430, Jul. 2012.

[3] W. Su, H. Eichi, W. Zeng, and M.-Y. Chow, "A survey on the electrification of transportation in a smart grid environment," *IEEE Trans. Ind. Informat.*, vol. 8, no. 1, pp. 1–10, Feb. 2012.

[4] I. Pavić, T. Capuder, and I. Kuzle, "Value of flexible electric vehicles in providing spinning reserve services," *Appl. Energy*, vol. 157, pp. 60–74, Nov. 2015.

[5] L. Hang, H. Zhang, S. Liu, X. Xie, C. Zhao, and S. Liu, "A novel control strategy based on natural frame for Vienna-type rectifier under light unbalanced-grid conditions," *IEEE Trans. Ind. Electron.*, vol. 62, no. 3, pp. 1353–1362, Mar. 2015.

[6] J.-S. Lee and K.-B. Lee, "Carrier-based discontinuous PWM method for Vienna rectifiers," *IEEE Trans. Power Electron.*, vol. 30, no. 6, pp. 2896–2900, Jun. 2015.

[7] A. Ali, M. Mansoor Khan, J. Yuning, Y. Ali, M. T. Faiz, and J. Chuanwen, "ZVS/ZCS Vienna rectifier topology for high power applications," *IET Power Electron.*, vol. 12, no. 5, pp. 1285–1294, May 2019.

[8] G. Rajendran, C. A. Vaithilingam, K. Naidu, and K. S. P. Oruganti, "Energy-efficient converters for electric vehicle charging stations," *Social Netw. Appl. Sci.*, vol. 2, no. 4, pp. 1–15, Apr. 2020.

[9] Y.-Y. Hong and M.-J. Liu, "Optimized interval type-II fuzzy controller-based STATCOM for voltage regulation in power systems with photovoltaic farm," *IEEE Access*, vol. 6, pp. 78731–78739, 2018.

[10] K. Y. Ahmed, N. Z. Bin Yahaya, V. S. Asirvadam, N. Saad, R. Kannan, and O. Ibrahim, "Development of power electronic distribution transformer based on adaptive PI controller," *IEEE Access*, vol. 6, pp. 44970–44980, 2018.
[11] S. Narula, B. Singh, and G. Bhuvaneswari, "Power factor corrected welding power supply using modified zeta converter," *IEEE J. Emerg. Sel. Topics Power Electron.*, vol. 4, no. 2, pp. 617–625, Jun. 2016.
[12] S. Vazquez, J. A. Sanchez, J. M. Carrasco, J. I. Leon, and E. Galvan, "A model-based direct power control for three-phase power converters," *IEEE Trans. Ind. Electron.*, vol. 55, no. 4, pp. 1647–1657, Apr. 2008.
[13] A. S. Al-Ogaili, I. B. Aris, R. Verayiah, A. Ramasamy, M. Marsadek, N. A. Rahmat, Y. Hoon, A. Aljanad, and A. N. Al-Masri, "A three-level universal electric vehicle charger based on voltage-oriented control and pulse-width modulation," *Energies*, vol. 12, no. 12, p. 2375, Jun. 2019.
[14] M. Malinowski, M. Jasinski, and M. P. Kazmierkowski, "Simple direct power control of three-phase PWM rectifier using space-vector modulation (DPC-SVM)," *IEEE Trans. Ind. Electron.*, vol. 51, no. 2, pp. 447–454, Apr. 2004.
[15] W. Qi, S. Li, S.-C. Tan, and S. Y. Hui, "Design considerations for voltage sensorless control of a PFC single-phase rectifier without electrolytic capacitors," *IEEE Trans. Ind. Electron.*, vol. 67, no. 3, pp. 1878–1889, Mar. 2020.
[16] S. Durgadevi and M. G. Umamaheswari, "Analysis and design of single phase power factor correction with DC–DC SEPIC converter for fast dynamic response using genetic algorithm optimised PI controller," *IET Circuits, Devices Syst.*, vol. 12, no. 2, pp. 164–174, Mar. 2018.
[17] Y. Gui, M. Li, J. Lu, S. Golestan, J. M. Guerrero, and J. C. Vasquez, "A voltage modulated DPC approach for three-phase PWM rectifier," *IEEE Trans. Ind. Electron.*, vol. 65, no. 10, pp. 7612–7619, Oct. 2018.
[18] H. Nian, Y. Shen, H. Yang, and Y. Quan, "Flexible grid connection technique of voltage-source inverter under unbalanced grid conditions based on direct power control," *IEEE Trans. Ind. Appl.*, vol. 51, no. 5, pp. 4041–4050, Sep. 2015.
[19] M. Moallem, B. Mirzaeian, O. A. Mohammed, and C. Lucas, "Multi-objective genetic-fuzzy optimal design of PI controller in the indirect field oriented control of an induction motor," *IEEE Trans. Magn.*, vol. 37, no. 5, pp. 3608–3612, 2001.
[20] H. Acikgoz, A. Kumar, H. Beiranvand, and M. Sekkeli, "Hardware implementation of type-2 neuro-fuzzy controller-based direct power control for three-phase active front-end rectifiers," *Int. Trans. Electr. Energy Syst.*, vol. 29, no. 10, Oct. 2019, Art. no. e12066.
[21] Y. Li and H. Zhao, "A space vector switching pattern hysteresis control strategy in Vienna rectifier," *IEEE Access*, vol. 8, pp. 60142–60151, 2020.
[22] E. Barbie, R. Rabinovici, and A. Kuperman, "Modeling and simulation of a novel active three-phase multilevel power factor correction front end—The 'Negev' rectifier," *IEEE Trans. Energy Convers.*, vol. 35, no. 1, pp. 462–473, Mar. 2020.
[23] H. Radmanesh and M. Aeini, "A two-stage isolated AC-DC converter for more electric aircraft," in *Proc. 11th Power Electron., Drive Syst., Technol. Conf. (PEDSTC)*, Feb. 2020, pp. 1–6.
[24] G. Aiello, M. Cacciato, G. Scarcella, G. Scelba, F. Gennaro, and N. Aiello, "Mixed signals based control of a SiC Vienna rectifier for on-board battery chargers," in *Proc. 21st Eur. Conf. Power Electron. Appl. (EPE ECCE Eur.)*, Sep. 2019. pp. P.1–P.9.
[25] F. Palomba, F. Gennaro, M. Pavone, N. Aiello, G. Aiello, and M. Cacciato, "Analysis of PCB parasitic effects in a Vienna rectifier for an EV battery charger by means of electromagnetic simulations," in *Proc. 21st Eur. Conf. Power Electron. Appl. (EPE ECCE Eur.)*, Sep. 2019, pp. 1–10.
[26] S. Liu, J. Jiang, and G. Cheng, "Research on vector control strategy of three phase VIENNA rectifier employed in EV charger," in *Proc. Chin. Control Decis. Conf. (CCDC)*, Jun. 2019, pp. 4914–4917.
[27] J. A. Anderson, M. Haider, D. Bortis, J. W. Kolar, M. Kasper, and G. Deboy, "New synergetic control of a 20kW isolated Vienna rectifier front-end EV battery charger," in *Proc. 20th Workshop Control Modeling Power Electron. (COMPEL)*, Jun. 2019, pp. 1–8.
[28] S. Prakash P, R. Kalpana, B. Singh, and G. Bhuvaneswari, "Design and implementation of sensorless voltage control of front-end rectifier for power quality improvement in telecom system," *IEEE Trans. Ind. Appl.*, vol. 54, no. 3, pp. 2438–2448, May 2018.
[29] J.-S. Lee, K.-B. Lee, and F. Blaabjerg, "Predictive control with discrete space-vector modulation of vienna rectifier for driving PMSG of wind turbine systems," *IEEE Trans. Power Electron.*, vol. 34, no. 12, pp. 12368–12383, Dec. 2019.
[30] H. Ma, Y. Xie, and Z. Shi, "Improved direct power control for Vienna-type rectifiers based on sliding mode control," *IET Power Electron.*, vol. 9, no. 3, pp. 427–434, Mar. 2016.
[31] A. E. Emanuel, "Summary of IEEE standard 1459: Definitions for the measurement of electric power quantities under sinusoidal, nonsinusoidal, balanced, or unbalanced conditions," *IEEE Trans. Ind. Appl.*, vol. 40, no. 3, pp. 869–876, May 2004.
[32] D. R. Espinoza-Trejo, E. Bárcenas-Bárcenas, D. U. Campos-Delgado, and C. H. De Angelo, "Voltage-oriented input-output linearization controller as maximum power point tracking technique for photovoltaic systems," *IEEE Trans. Ind. Electron.*, vol. 62, no. 6, pp. 3499–3507, Nov. 2014.
[33] R. Ottersten, "On control of back-to-back converters and sensorless induction machine drives," Chalmers Univ. Technol., Gothenburg, Sweden, Tech. Rep. 450, 2003.
[34] M. A. A. M. Zainuri, M. A. M. Radzi, A. C. Soh, N. Mariun, and N. A. Rahim, "DC-link capacitor voltage control for single-phase shunt active power filter with step size error cancellation in self-charging algorithm," *IET Power Electron.*, vol. 9, no. 2, pp. 323–335, Feb. 2016.
[35] Y. Hoon, M. Mohd Radzi, M. Hassan, and N. Mailah, "DC-link capacitor voltage regulation for three-phase three-level inverter-based shunt active power filter with inverted error deviation control," *Energies*, vol. 9, no. 7, p. 533, Jul. 2016.
[36] R. Gowthamraj, C. Aravind, and O. Prakash, "Modeling of Vienna rectifier with PFC controller for electric vehicle charging stations," in *Proc. AIP Conf.*, vol. 2137, no. 1, 2019, Art. no. 030003.
[37] M. Zhang, L. Hang, W. Yao, Z. Lu, and L. M. Tolbert, "A novel strategy for three-phase/switch/level (Vienna) rectifier under severe unbalanced grids," *IEEE Trans. Ind. Electron.*, vol. 60, no. 10, pp. 4243–4252, Oct. 2013.
[38] S. Durgadevi and M. G. Umamaheswari, "Adaptive neuro fuzzy logic controller based current mode control for single phase power factor correction using DC-DC SEPIC converter," in *Proc. Int. Conf. Power Embedded Drive Control (ICPEDC)*, Mar. 2017, pp. 490–495.
[39] P. Xiong and D. Sun, "Backstepping-based DPC strategy of a wind turbine-driven DFIG under normal and harmonic grid voltage," *IEEE Trans. Power Electron.*, vol. 31, no. 6, pp. 4216–4225, Jun. 2016.

GOWTHAMRAJ RAJENDRAN received the Bachelor of Engineering degree from the Government College of Engineering, Salem, India, in 2014, and the Master of Engineering degree (Hons.) from the PSG College of Technology, Coimbatore, India. He is currently pursuing the Ph.D. degree in electrical engineering with Taylor's University, Malaysia. His current research is focused on the ac-dc power converters for electric vehicle charging stations. His research interest includes high-frequency semiconductor devices (Silicon Carbide and Gallium Nitride) for power converters in electric vehicle charging stations. He is working under the research cluster VERTICALS aligned with SDG goals on sustainable energy and mobility (SDG 7, 11).

CHOCKALINGAM ARAVIND VAITHILINGAM (Senior Member, IEEE) received the B.Eng. degree from Bharathiyar University, India, in 1998, the M.Eng. degree from Bharathidasan University, India, in 2001, and the Ph.D. degree in electrical power engineering from the Universiti Putra Malaysia, in 2013. He is heading the Electrical and Electronic Engineering Programme, Faculty of Innovation and Technology, Taylor's University Malaysia and heading the research cluster VERTICALS aligned with SDG goals on sustainable energy and mobility (SDG 7, 11). He is a very frequent speaker at various international and national platforms. He is also a Professional Technologists with the Malaysian Board of Technologists. He is a member of IET, U.K. He is a member of the Society of Engineering Education Malaysia. He is a registered Chartered Engineer registered professional with the Engineering Council, U.K.

NORHISAM MISRON (Member, IEEE) received the B.Eng., M.Eng., and Dr.Eng. degree in system engineering from Shinshu University, Nagano, Japan, in 1998, 2000, and 2003, respectively. He joined the Department of Electrical and Electronic Engineering, Universiti Putra Malaysia, as a Lecturer, in 2003, where he became an Associate and a Full Professor, in 2009 and 2016, respectively. He is currently an Associate Researcher with the Institute of Advance Technology (ITMA) and Institute of Plantation Study (IPS). His research interest includes magnetic application, including sensor and electrical machine development. His current research focuses on the design and development of agricultural sensor and actuator devices for the oil palm industry, including magnetic gear, high torque density motor, and fruit battery sensors. He serves on various technical committees of IEEE.

KANENDRA NAIDU received the master's and Ph.D. degrees in electrical engineering from the University of Malaya, in 2011 and 2015, respectively. He is currently a Senior Lecturer with the Universiti Teknologi MARA (UiTM), Shah Alam. His research interest includes electrical engineering specializing in the implementation of artificial intelligence in power systems. He also has strong working experience in a variety of evolutionary and swarm-based optimization techniques, graph theory, wavelet transform, and artificial neural networks.

MD RISHAD AHMED received the B.Sc. degree from the Bangladesh University of Engineering and Technology (BUET), Dhaka, Bangladesh, in 2011, and the M.Sc. degree (Hons.) and the Ph.D. degree from The University of Manchester, Manchester, U.K., in 2013 and 2017, respectively. From September 2013 to February 2014, he worked as a Research Assistant with Cardiff University in the Control Techniques Multilevel Drive Research Project. Since September 2017, he has been working as a Design Engineer of automotive power electronics with Dynex Semiconductor, U.K. In Dynex, he led the research and development of onboard charger and dc-dc converter products for electric vehicles. He joined the University of Nottingham, as an Assistant Professor of power electronics, in March 2020. His research interests include wideband-gap semiconductor devices, passive components, converter packaging, and high-frequency converters.